Journal of Chromatography, 175 (1979) 269–281

CHROM. 11,871

DUAL-DETECTOR–POST-COLUMN REACTOR SYSTEM FOR THE DETECTION OF ISOENZYMES SEPARATED BY HIGH-PERFORMANCE LIQUID CHROMATOGRAPHY

I. DESCRIPTION AND THEORY

JOE A. FULTON, TIMOTHY D. SCHLABACH, JAMES E. KERL and E. CLIFFORD TOREN, Jr.*

Department of Pathology, University of South Alabama, Mobile, Ala. 36688 (U.S.A.)

and

ARNOLD R. MILLER

Institute on Aging, University of Wisconsin, Madison, Wisc. 53706 (U.S.A.)

(First received January 22nd, 1979; revised manuscript received March 23rd, 1979)

SUMMARY

We describe a dual-detector–post-column chromatographic reaction detector system that corrects for substances present in biological samples that interfere with the measurement of isoenzymes separated on a chromatographic column. The response observed at the detector in front of the reaction coil is mathematically dispersed, time transformed and subtracted from the detector behind the coil to produce a blank corrected chromatogram. The same computer program calculates peak areas and other chromatographic parameters such as height equivalent to a theoretical plate and retention time. In addition, we have evaluated the dispersion effects caused by various changes in our experimental system.

INTRODUCTION

The rapid, quantitative measurement of isoenzymes remains a difficult but important problem in clinical chemistry. We have recently reported[1] a post-column reactor (PCR) system for the detection and quantitation of lactate dehydrogenase (LD) isoenzymes. The PCR was a coil of narrow-bore, stainless-steel tubing. The column effluent and the LD assay reagent were combined in a Tee-connection and passed through the coil where the enzymatic reaction occurred.

Regnier and co-workers[2,3] have used a packed bed reactor instead of a tubular reactor for the analysis of the LD isoenzymes. We found, however, that the void volume of such a reactor can increase after prolonged use at high pH. Since it was

* To whom correspondence should be addressed.

important in our work to have a reactor of constant internal volume, we chose a tubular reactor.

Both systems[1,2] used a single detector placed behind the reactor to measure the absorbance or fluorescence of the enzymatic product, NADH (nicotinamide adenine dinucleotide-reduced form). These systems operate satisfactorily for samples containing purified LD isoenzymes or serum samples having substantial LD activity. However, most sera contain materials that interfere with the detection of NADH by absorbing at 340 nm or fluorescing like NADH with an excitation around 340 nm. These interferences can obscure the resolution and restrict the quantitation of some NADH peaks. Kessler *et al.*[4] also observed interferences at 340 nm which necessitated blank measurements by substituting buffer for NAD (nicotinamide adenine dinucleotide) as a sample blank.

The objective of this work is to develop and characterize a dual-detector system to compensate for endogenous interferences. This system will allow automated, rapid procedures to be used so that isoenzymes can be measured continuously as they elute from a column.

Obviously, the contribution of endogenous interferences to peaks of enzyme activity can be minimized by allowing the enzyme reaction to generate a sufficiently large concentration of product relative to the level of background interference present in the sample. However, since serum LD activities vary widely and the amount of background interference in serum samples varies, different reactor sizes would be necessary to maintain optimum conditions for a wide range of samples. Our post-column detection system was designed to overcome this problem and permit one tubular reactor to be used for a broad spectrum of samples.

The design of this post-column detection system is similar to the LD channel in the SMAC™ (Technicon Instruments, Tarrytown, N.Y., U.S.A.)[5]. Both systems use a pre-reaction detector (placed before the reactor) to subtract sample absorbance from the response of the detector at the reactor exit. Although we did not have a Technicon SMAC™ or AutoAnalyzer™ to evaluate, it would have been necessary to achieve a very high sampling rate for the point-by-point subtraction of sample interference(s).

EXPERIMENTAL

The apparatus used in these studies is shown in Fig. 1. The absorbance data from the detectors (A_{340} unless otherwise indicated) were acquired with a DEC Model 11/V03 computer with 24K words of memory (Digital Equipment Corp., Maynard, Mass., U.S.A.). A DEC GT-46 graphics computer system equipped with a Cøpløt plotter (Houston Instruments, Houston, Texas, U.S.A.) was used for data reduction. Software was written in Fortran IV under the RT-11 version[3] operating system.

Solutions of NADH were prepared from spectral calibration standards (Sigma, St. Louis, Mo., U.S.A.) by dilution with 20 m*M* Tris–HCl buffer (pH 8.0). This buffer was also used to fill the reservoirs of the main and reagent pumping units.

Theory of operation

Since serum samples contain many proteins at much higher concentrations than any serum enzyme, direct absorbance detection of a particular enzyme is not

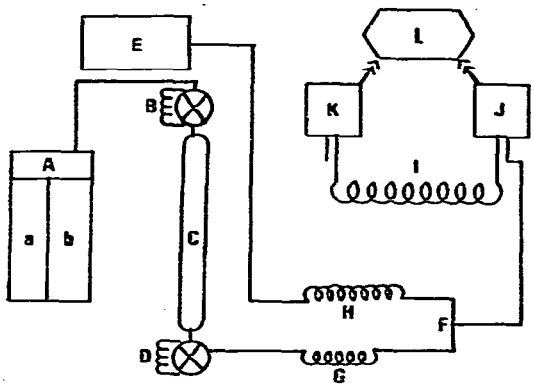

Fig. 1. Schematic diagram of HPLC and post-column enzyme reactor. A Varian Model 8500 gradient high-performance liquid chromatograph (Varian Instrument Division, Palo Alto, Calif., U.S.A.) was the main gradient pumping unit, A. Rheodyne 7120 injector valves (Altex, Berkely, Calif., U.S.A.) with 100-μl loops were installed for pre- and post-column injection, B and D. The reagent pump, E, was a Spectra-Physics Model 3500 (Spectra-Physics, Santa Clara, Calif., U.S.A.), E. C was the separation column. The mixing Tee, F, was a standard 0.16-cm stainless-steel Swagelok tee (Altech, Houston, Texas, U.S.A.). The predector delay coil, G, the coil to bring the reagent up to temperature, H, and the delay coil (1968 cm), I, were stainless-steel tubing with an I.D. of 0.05 cm. A Waters Assoc. Model 440 dual absorbance detector with 340-nm filters (Waters Assoc., Milford, Mass., U.S.A.) was used at points J and K. The detector electronics is module L.

possible. Serum enzymes, therefore, can only be detected by their catalytic activity. LD catalyzes the oxidation of L-lactate to pyruvate as shown:

$$\text{L-lactate} + \text{NAD}^+ \underset{\longleftarrow}{\overset{\text{LD}}{\longrightarrow}} \text{pyruvate} + \text{NADH} + \text{H}^+$$

The rate of the enzymatic reaction is determined by measuring the increase in NADH concentration with time, which can be obtained from the increase in absorbance, ΔA, at 340 nm. For a fixed time interval, T, ΔA is directly proportional to enzyme activity provided that the reaction is governed by zero order kinetics over the interval. The response of detector 2 (Fig. 1) is a direct measure of ΔA in the absence of baseline drift and sample interferences. The time interval, T, is fixed by the flow-rate through the PCR coil and the internal volume of the coil.

When sample interferences are present, it is necessary to subtract out their contribution to the response at detector 2 (K, Fig. 1). To accomplish this, detector 1 (J, Fig. 1) was placed after the mixing Tee but before the reaction coil. Detector 1 measured the absorbance of the solution passing through the coil before the enzyme reaction could produce any detectable NADH. It also responded to non-reacting interferences which elute from the column. A direct subtraction of the readings at detector 1 from detector 2 is not possible because the output of detector 1 precedes that of detector 2 by the delay time, T (reactor residence time), and because non-reacting interference peaks observed at detector 1 will be dispersed in the reaction coil before they reach detector 2. Dispersion causes the peak's standard deviation to increase, which results in peaks that are wider and have reduced peak heights, but dispersion does not affect the peak areas which remain the same.

We have developed a computer algorithm based on an empirical model which transforms peaks with respect to time and peak shape so that interferences observed at detector 1 can be directly subtracted, point-by-point, from the readings at detector 2 to produce a chromatogram that has been corrected for sample interferences and drifts in baseline.

Program operation

The data reduction subroutines smooth the digitized chromatographic data, evaluate the first and second derivatives of the data, find local maxima and minima, integrate the peaks of the chromatogram, simulate dispersion occurring in the PCR (delay coil), and compensate for the delay time, T. These subroutines also plot the data, determine peak parameters such as area, retention time, peak height, resolution and height equivalent to a theoretical plate (HETP). Subroutines are written in Fortran IV with most arguments passed in common. With this structured program approach, the main driver programs are kept very short. Because of the ease of restructuring, the main programs can be easily changed without rewriting the subroutines, thus the entire program is very flexible.

The flow chart for the data acquisition program, LCD (Liquid Chromatography Data), is straightforward and is shown in Fig. 2. This program tests the chromatographic system, *i.e.* the gradient controls, the injection start flag, etc. The program starts, stops, and holds the gradient of the chromatograph, acquires the absorbance data from the two detectors, smooths the data with a 5-point, box-car smooth, outputs a copy of the chromatographic data to a cathode ray tube screen, can plot the data on a teletypewriter device and stores the data on floppy disk.

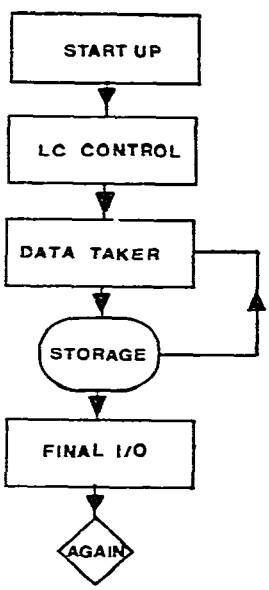

Fig. 2. Flow chart of the HPLC control and data acquisition program, LCD.

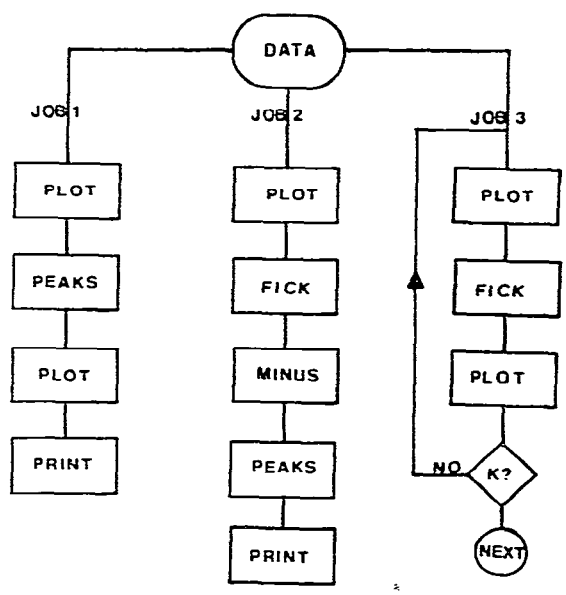

Fig. 3. Flow chart of the SAVAY data reduction program. Order of and subroutines called by each Job (1–3) are shown.

The data so acquired are passed to the SAVAY program (Savitzky–Golay)[6], a flow chart of which is shown in Fig. 3. The SAVAY program is the main driver and calls subroutines using the acquired data to perform three main jobs:

(1) Smooths and differentiates the raw data by the Savitzky–Golay[6] method, finds peaks, troughs and areas under peaks, plots the data and calculates the previously described parameters.

(2) Simulates peak dispersion from detector 1 with an equation analogous to Fick's Law, subtracts these transformed data from that of detector 2, plots the corrected chromatogram and prints out the corrected areas.

(3) Allows empirical dispersion constants to be determined by applying the dispersion transform on the experimental data set, finds peaks, troughs, and areas, plots the original data set and overplots the transformed data set. It also finds the best dispersion coefficient for non-reacting peaks by evaluating a series of coefficients for the goodness of fit between the transformed data from detector 1 and the data from detector 2.

The operations of greatest interest are the smoothing, differentiation, dispersion-simulation, time-transformation and peak-finding procedures. Smoothing and differentiation are accomplished by the Savitzky–Golay method[6]. The peak-finding routine is composed of two sections: a peak envelope detection routine and an overlap peak detector. A peak envelope is determined by the number of points above the baseline. When five points in a continuous series are above a preset threshold, the detection program assumes that a peak envelope has been found and stores the first point's position. Points are checked until three points below the threshold are found. The envelope's starting and ending points are passed to the overlap detector. Checks are made to see if a single peak or overlapping peaks are present. Overlapping peaks are then separated by dropping a perpendicular from the intermediate minimum (valley). The peak-detector routine is based on finding the zeroes of the chromatogram's first derivative. Zeroes are found by an inspection procedure based on the signs of the derivative, *i.e.*, if a function, for which only discrete, equally spaced points is evaluated, and has opposite signs at points $i-1$ and $i+1$, then the derivative at point i is assumed to be zero.

Transformation method for blank correction

The purpose of this procedure is to numerically disperse the data collected at detector 1. This procedure is used to predict the response profile attributable to interferences at the final detector from the response at the initial detector before any reaction occurs. The subtraction results in a profile, representing only the reaction products.

We assumed that an equation analogous to Fick's Second Law would govern the dispersion of the solute in a flowing stream, as did Grushka *et al.*[7] and Ruzicka and Hansen[8].

$$\partial C/\partial t = D\partial^2 C/\partial x^2 - u\partial C/\partial x \qquad (1)$$

Eqn. 1 is not restricted to any particular type of function and can be used to disperse peaks of any shape. The assumption is made, however, that the concentration profile, obtained at uniform time intervals at the detector, is equivalent to the concen-

tration profile with respect to distance when the sample component produces a detector response. This assumption is substantiated by the relation, $x = ut$, where u is the constant linear velocity, therefore, $dx = u dt$ and $dx^2 = u^2 dt^2$. After making these substitutions, eqn. 1 then becomes:

$$\frac{dC}{dt} = K' \cdot \frac{d^2C}{dt^2} \tag{2}$$

where K' is the empirical dispersion constant ($D/2u^2$).

Eqn. 2 can be readily solved by the computer program, since the response of the analog-to-digital converter, which monitors the absorbance detector, is directly proportional to concentration. When the detector response is substituted for concentration, eqn. 2 becomes:

$$\frac{dR}{dt} = K \cdot \frac{d^2R}{dt^2} \tag{3}$$

The smoothed, second partial derivative of R, $\bar{R}''_i$, is calculated for each data point, i, by the 5-point Savitsky-Golay[6] convolution algorithm and stored. Eqn. 3 must then be solved for each point in the data set using Euler's method[9]:

$$R_{i+1} = K \cdot \bar{R}'' + R_i \tag{4}$$

where R_i is the original response, $\bar{R}''_i$ is the smoothed, second derivative at point i and R_{i+1} is the predicted data point at one time interval, Δt, advanced from the time at which that point was read at the detector. In order to fully disperse the original data set, eqn. 4 must be solved for each point in the data set in an iterative manner. There must be $T/\Delta t$ iterations made to predict the totally dispersed response profile that should exist at time T advanced from the original collection time of the data set. Since T is the delay time between the two detectors (or the residence time of a sample component in the reaction coil), the transformation of the data collected at detector 1 results in a totally dispersed response profile. This is the predicted response for the original data set at detector 2.

This effect of iterations on peak spreading is shown in Fig. 4. The spreading of the original data set (trace A) increases dramatically with the number of iterations performed. As the number of iterations is increased, more points that were originally on the baseline become elevated and incorporated into the dispersed peaks. Since the sign of the second derivative for points near the baseline (concave up) is positive, successive iterations of eqn. 4 elevate these points. Thus, successive iterations cause peak boundaries to increase, resulting in peak spreading.

A more elaborate solution to eqn. 4, such as the Runge–Kutta method[10] was not used because many more time consuming computations would be required. Our procedure already requires $m(T/\Delta t)$ computations, where m is the number of points in the data set. Typically, we collect 1200 points at 2-sec intervals when we determine an LD isoenzyme profile. Since the delay time in the PCR is usually 80 sec, our model already requires 48,000 solutions to fully disperse the data set.

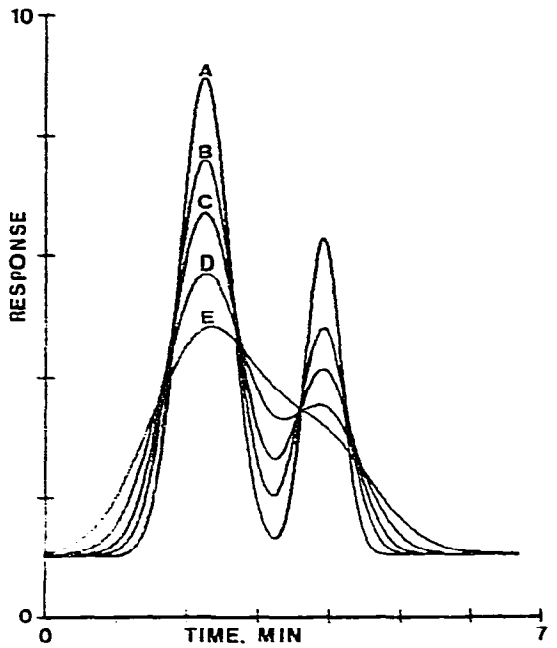

Fig. 4. Effect of increasing the number of iterations and the delay time on peak dispersion. A 1200-point simulated chromatogram (trace A) was transformed for the following times (and iterations): B, 300 sec; C, 600 sec; D, 1200 sec and E, 2400 sec. K was the same for each trace and was 0.30 sec.

For ease in programming, the time transformation of the dispersed data set is accomplished by a separate subroutine. To each of the m points in the data set, the delay time, T, is added, and the points beyond m are discarded. Since all the points in the array have been advanced $T/\Delta t$ positions, new points must be generated to fill these vacant positions. These positions are filled with the mean value of the first $T/\Delta t$ points before the time transformation. The dispersed, time transformed data set is stored for the subsequent subtraction from the data set collected at detector 2 (Job 2). The subtraction subroutine also corrects for any difference in offset between detectors 1 and 2.

RESULTS AND DISCUSSION

We did three basic types of experiments: (1) used the program to disperse simulated data sets and removed simulated interferences, (2) tested the program on experimental data and (3) determined the effect of flow-rate on dispersion.

Simulations

Fig. 5. shows the functions of Jobs 1 and 2. Trace A was produced by Job 1, and it is a plot of the data simulating the response of detector 2. Trace B is a plot of the data simulating the response of detector 1. Trace C is the result of the subtraction of B from A after B has been dispersed and time-transformed. Thus, trace C represents the corrected chromatogram after removal of the background peaks. In Fig. 6 the chromatographic parameters are listed for trace A and C. Note that in trace C the

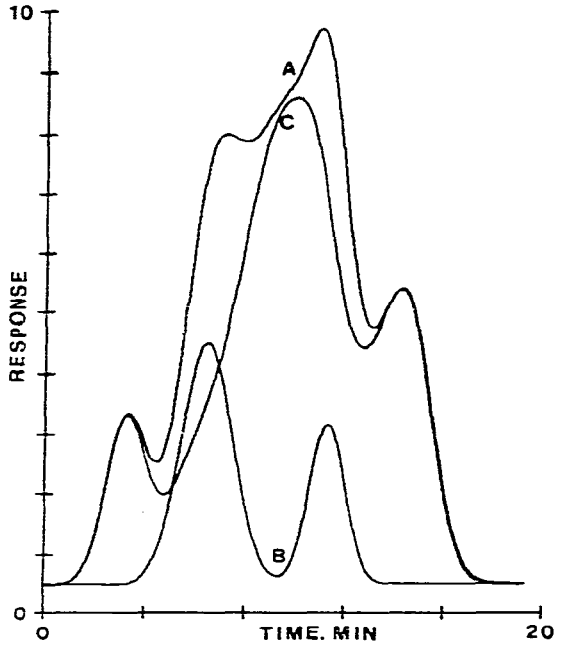

Fig. 5. Illustration of Jobs 1 and 2 using a 1200-point simulation. The chromatogram in trace A represents the output of detector 2. Trace B represents the output of detector 1. Trace C is the result of the point-by-point subtraction of trace B from trace A after trace B has been dispersed with a K of 0.30 sec and time-transformed for a 60-sec interval.

PLOT A

#	R TIME	HEIGHT	% AREA	IN STD	AREA
1	0.85	2.65	7.35	1.00	64.6
2	1.83	6.12	25.00	3.42	220.0
3	2.82	7.43	51.67	7.03	454.0
4	3.67	4.20	15.98	2.17	140.0

PLOT C

#	R TIME	HEIGHT	% AREA	IN STD	AREA
1	0.85	1.83	8.42	1.00	43.9
2	2.72	4.52	73.52	8.73	383.0
3	3.68	2.86	8.06	2.15	94.1

Fig. 6. Data reduction of trace A and trace C of Fig. 5.

overlapping peaks have been deconvoluted so that the true areas of the three peaks are obtained.

Job 3 is primarily used to obtain suitable values for K. Fig. 7 illustrates the overplotting capability of this program which plots the data on a graphics scope and provides hardcopy on request. A suitable K value can be chosen by trial-and-error, with visual matching of trace B with A, where trace A represents the response at detector 2 and trace B represents the dispersed and time-transformed response of detector 1.

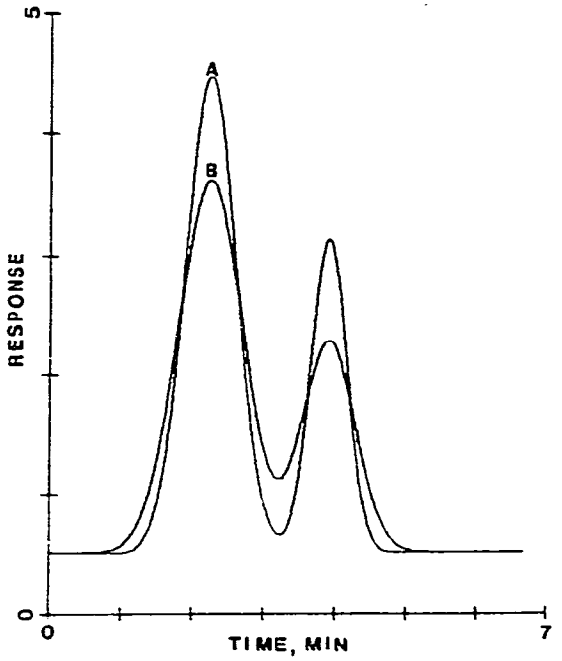

Fig. 7. Illustration of Job 3. Trace A is a 400-point, simulated chromatogram representing the output of detector 2. Trace B represents the dispersed ($K = 0.30$ sec) and time-transformed output of the simulated data from detector 1 using a delay time of 120 sec.

The simulated effect of varying the delay time, T, was shown in Fig. 4. As expected, the original peaks broaden and finally coalesce to one peak, appearing as a single "tailing" peak. The curves in Fig. 4 are in agreement with the expected results for the decrease in resolution with increased peak spreading.

Experimental results

The computer algorithm was tested by injecting NADH into the system to represent a nonreacting interferent. A 100-μl aliquot of 24.1 μM NADH was injected at position B (Fig. 1). The chromatographic column was replaced by a 518 $\times$ 0.076 cm coil of stainless-steel tubing. This coil was used to generate a nearly Gaussian input peak under isocratic conditions with 20 mM Tris buffer (pH 8.0). The responses of detectors 1 and 2 to the injected NADH are shown in Fig. 8 as peaks A and B, respectively. Peak B is seen to be wider and shorter than peak A, but the peak areas were found to be the same. The first three moments were determined for each peak accord-

ing to the methods of Grushka *et al.*[11]. The variance and skew for peak A were found to be 160.4 sec^2 and 0.376, respectively, while the variance and skew for peak B were found to be 210.0 sec^2 and 0.304, respectively. The delay time was calculated from the time difference between the peak centroids and was 79 sec.

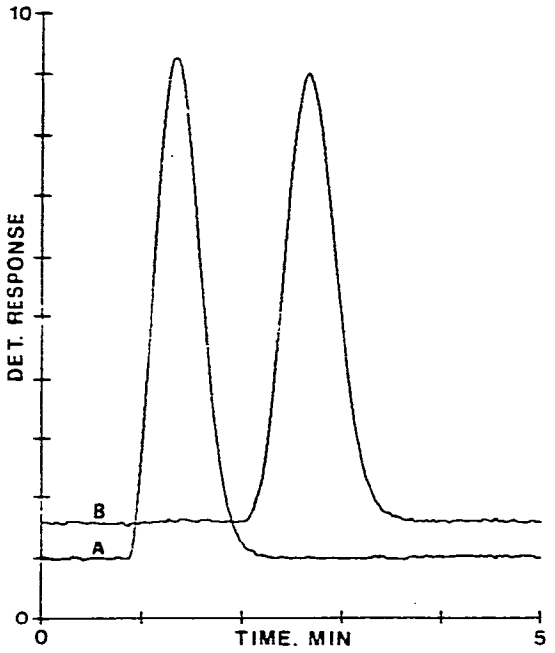

Fig. 8. Response of detectors 1 and 2 to a non-reacting NADH peak. A 100-μl aliquot of 24.1 μM NADH was injected at C (Fig. 1). The flow-rate from A was 2.0 ml/min and from E was 1.0 ml/min producing a flow-rate of 3.0 ml/min through the reaction coil and a residence time of 79 sec. Trace A is the NADH peak observed at detector 1 while trace B is the NADH peak observed at detector 2. The traces were separated by 0.5 response units for clarity.

Fig. 9 illustrates how the computer algorithm corrects for a non-reacting interferent. Trace B (Figs. 8 and 9) is the smoothed response of detector 2, and trace A′ (Fig. 9) is the dispersed and time-transformed response of detector 1. It is apparent that the two traces are nearly identical. The point-by-point subtraction of trace A′ from B, results in a nearly flat baseline, trace C. The very shallow, sinusoidal curve in trace C represents the error in matching peak A′ with peak B. This error was determined to be less than one percent, when the area of this sinusoidal curve was compared to the area of peak B.

Dispersion

The dispersion (band spreading) of a peak in a coil of tubing has been reported to vary with flow-rate[8]. Dispersion of a peak (or solute band) in an open tube is caused primarily by convective mixing due to flow inequalities in the tube. Flow inequalities also occur in a coil of tubing, and for a given coil, they are dependent on flow-rate and solvent viscosity.

The effect of flow-rate on dispersion was studied by injecting a 100-μl aliquot

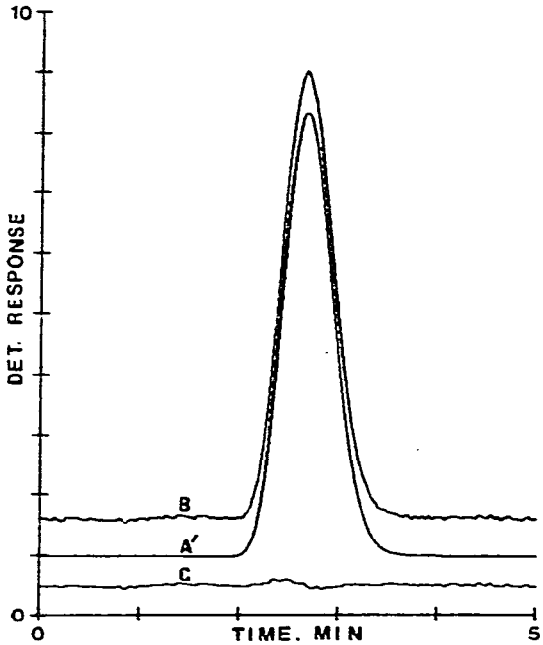

Fig. 9. Comparison of the predicted and observed response profiles at detector 2. Trace A′ is the dispersed (K = 0.303 sec) and time-transformed profile of the response from detector 1 (see trace A in Fig. 8) using a 79-sec delay time. Trace B (also shown in Fig. 8) is the response profile observed at detector 2 . Trace C is the result of the point-by-point subtraction of trace A′ from trace B. Trace C was elevated 0.5 response units from the axis for clarity.

of 9.6 μM NADH. Again the 518 × 0.076 cm coil was substituted for the chromatographic column (Fig. 1) to produce a Gaussian input peak. The reagent pumping system was not used in these studies and the Tee connector (F in Fig. 1) was replaced with a 0.16-cm union. The overall flow-rate was controlled by the Varian 8500 high-performance liquid chromatograph (A in Fig. 1).

Dispersion of a solute band in an empty coil of tubing can be expressed in terms of increased band variance, or it can be simply expressed as the dispersion number which is the ratio of the peak height as.the peak enters the coil to the peak height at the coil exit[8]. For Gaussian peaks this ratio is simply the ratio of the standard deviation of the peak as it leaves the coil to the standard deviation of the peak at the coil entrance. This ratio indicates the loss in peak response and the increase in peak volume which is attributable to dispersion (band spreading) in the coil. The peak heights at detectors 1 and 2 were determined from the digitized absorbance data by determining a baseline from the best fit between 50 points on either side of the peak. The standard deviation for each peak was determined from the square root of the peak variance.

The effect of flow-rate on dispersion is shown in Table I. The peak height ratio shows an irregular increase in dispersion with flow-rate, while the ratio of the standard deviation for each peak shows a more gradual increase in dispersion with flow-rate. Although the flow-rate was increased three-fold, dispersion in the coil only increased 1.1-fold. When the coil is used as a PCR, slowing down the flow-rate through

TABLE I

DISPERSION COMPARISON

All data were obtained from the mean of duplicate measurements.

Flow-rate (ml/min)	*Dispersion number*[a]	*Standard deviation (sec)*		σ_B/σ_A	*K (sec)*
		Peak A	*Peak B*		
1.00	1.37	22.6	29.1	1.29	0.978
1.51	1.37	15.9	21.2	1.35	0.749
2.02	1.39	12.1	16.6	1.37	0.638
2.52	1.47	9.14	12.9	1.41	0.560
3.04	1.47	7.46	10.7	1.43	0.404

[a] Ratio of peak heights at detector 1 (A) to detector 2 (B).

the coil from 3 to 1 ml/min would only reduce peak overlap by 10% while increasing detection time three-fold under these conditions.

The values of K required to transform the peaks at detector 1 are listed in Table I. These values are seen to decrease substantially with flow-rate. Slower flow-rates produce peaks which have greater peak widths, although the amount of NADH contained in these peaks remains unchanged. Since the peaks are wider, the response profile changes more gradually with respect to time. Since the second derivative is the rate of change of the first derivative, it changes even more gradually at slower flow-rates. Therefore, larger values of K were necessary to compensate for the substantial decrease in magnitude of the second derivative in eqn. 4 which occurred at slower flow-rates. It has also been observed in other experiments that broader peaks require larger values of K to be adequately dispersed by the computer algorithm.

The optimum value of K was chosen for each data set by minimizing the area of the sinusoidal curve (see trace C, Fig. 9) that results from the subtraction of the dispersed and time-transformed data set from the response at detector 2. It was observed that inappropriate K values result in sinusoidal curves of varying amplitudes, but that the positive and negative portions of the curve tend to be similar in magnitude. The determination of peak areas after the background subtraction (see trace C, Fig. 4) should not be greatly affected by inappropriate K values since the negative and positive contributions to peak areas tend to cancel.

CONCLUSIONS

We have used an empirical model to numerically disperse peaks. It was assumed that the rate of change in the response profile, caused by dispersion in the reaction coil, is proportional to the second derivative of the response profile. The rate of change over one time interval is determined from the second derivative which is added, point-by-point, to the previous profile to produce a new response profile. By repeating this procedure for a sufficient number of time intervals, it is possible to numerically estimate the output profile, resulting from dispersion in a coil of tubing having a delay time, T. For a predetermined delay time, the above procedure is repeated $T/\Delta t$ times.

We have developed this model primarily to treat interferences present in serum samples which are detected before a PCR coil. These interferences must be subtracted

from the response of the detector at the coil outlet, which measures the amount of reaction product formed in the PCR. We have shown in this paper how this method disperses peaks and can be used to predict the shape of a non-reacting peak after it has been dispersed in the reaction coil. In our next paper we show the application of this method to the subtraction of serum interferences from peaks produced by the activity of lactate dehydrogenase isoenzymes after they have been separated by high-performance liquid chromatography[12].

Program listings can be obtained from the authors on request. Alternatively, source programs will be furnished with requestor-supplied, formatted, DEC, RT-11, compatible floppy disk.

ACKNOWLEDGEMENTS

Early work was supported by Grant GP-43624X from the National Science Foundation. The project was mainly supported by Grant GM 24452 from the National Institutes of Health. The authors acknowledge the helpful discussions with Hal Brand of the Lawrence Livermore Laboratory.

REFERENCES

1 R. R. Schroeder, P. J. Kudirka and E. C. Toren, Jr., *J. Chromatogr.*, 134 (1977) 83.
2 T. D. Schlabach, S. H. Chang, K. M. Gooding and F. E. Regnier, *J. Chromatogr.*, 134 (1977) 91.
3 T. D. Schlabach, A. J. Alpert and F. E. Regnier, *Clin. Chem.*, 24 (1978) 1351.
4 G. Kessler, R. L. Rush, L. Leon, A. Delea and R. Cupiola. *Advances in Automated Analysis, Technicon International Congress 1970, Vol. I, Clinical Analysis*, Thurman Associates, Miami, Fla., 1971, p. 67.
5 *Technicon SMAC, High-Speed, Computer-Controlled Biochemical Analyzer, Vol. II, Methods*, Technical Publication No. UA3-0306B2, Technicon Instruments Corp., Tarrytown, N.Y., Section XVI, September, 1976.
6 A. Savitzky and M. J. E. Golay, *Anal. Chem.*, 36 (1964) 1639.
7 E. Grushka, L. R. Snyder and J. H. Knox, *J. Chromatogr. Sci.*, 13 (1975) 25.
8 J. Ruzicka and E. H. Hansen, *Anal. Chim. Acta*, 99 (1978) 37.
9 D. M. Young and R. T. Gregory, *A Survey of Numerical Mathematics*, Vol. I, Addison-Wesley, Reading, Mass., 1972, pp. 441–449.
10 R. L. Hetter and S. P. Prowel, Jr., *Modern Methods of Engineering Computations*, McGraw-Hill, New York, N.Y., 1969, pp. 268–278.
11 E. Grushka, M. N. Meyers, P. D. Schetter and J. C. Giddings, *Anal. Chem.*, 41 (1969) 889.
12 J. A. Fulton, T. D. Schlabach, J. E. Kerl and E. C. Toren, Jr., *J. Chromatogr.*, 175 (1979) 283.